Active NPC Converter for Variable Speed Operation of Pumped Storage Hydropower Plant

Raghbendra Tiwari
Dept. of Electric Power Engineering
NTNU
Trondheim, Norway
raghbendra.tiwari@ntnu.no

Roy Nilsen
Dept. of Electric Power Engineering
NTNU
Trondheim, Norway
roy.nilsen@ntnu.no

Arne Nysveen
Dept. of Electric Power Engineering
NTNU
Trondheim, Norway
arne.nysveen@ntnu.no

Abstract—**This paper discusses the full size Active Neutral Point Clamped (ANPC) Converter for large scale (100 MW, 13–15 kV) synchronous machine in a pumped storage hydropower application to enable the variable speed operation. Such a converter provides the flexibility of fast transition of modes from pumping to generating or vice versa. This allows an easy integration of renewable energy sources to the grid. While starting the machine in pump mode, a very high starting torque is required if submerged in water. Two alternative converter configurations, namely, NPC and ANPC have been studied in this paper. These converter topologies are compared with regard to their capabilities in providing starting torque in pump mode. The loss distribution amongst the semiconductor devices has been presented using IGCT as the switching device. The results based on analytical calculations show that ANPC converter provides over 80% higher starting torque compared to NPC converter which is an essential requirement for this application.**

Index Terms—**Active Neutral Point Clamped Converter, Analytical loss calculation, Medium-voltage drives, Pumped Storage Hydropower, Variable Speed Drives**

I. INTRODUCTION

At present, the pumped storage hydropower plants are realized with a reversible pump-turbine (RPT) and an AC machine (generator/motor) connected on the same shaft. In most of the pumped storage plants, the AC machine is the synchronous machine directly connected to the grid and therefore, the set of machines run at almost constant speed depending upon the frequency of the grid regardless of the amount of water flow into the turbine/pump. However, it is a well-proven theory that the turbine/pump operates at optimal efficiency only if its speed is varied according to the variation in the water flow. This optimal efficiency operation of hydraulic machines is currently being achieved in several power plants around the world with the help of Doubly Fed Induction Machine (DFIM) where a frequency converter of approximately 10–25% capacity of the stator rating is required to achieve variation of ± 10% in speed [1]. Even though, the system is widely used for few decades, it cannot dynamically switch the operation from generating mode to pumping mode or vice versa which is an important requirement to balance the ever-increasing amount of renewables being introduced to the grid.

In addition, it takes a long starting procedure in pump mode as the water in the turbine casing needs to be evacuated using an air compressor and a small ponny motor or soft starter is used to rotate the machine close to the synchronous speed. Such a dynamic mode switching from turbine to pump and vice versa can be achieved by decoupling the turbine/generator sets from the AC grid using a full power back-to-back converter between the AC machine and the grid using converter fed synchronous machine (CFSM). Such full size converter also needs to deliver high starting torque for a fast starting time of 10–30 seconds compared to 5–10 minutes as of today with existing technology of DFIM and auxiliary starting equipment. This technology needs a converter of the same rating as of the stator and therefore, the application can be limited by the size of the converter.

In the existing pumped storage power plants, the water from the turbine housing is blown away by an air compressor to ease the start up such that only an additional small-size machine is required to start the machine in pump mode. In this case, starting torque required to drive the pump–turbine system is 3–6% of the torque at rated synchronous speed. For a fast startup, it is required to run the system with water in the casing. In such situation, the load torque produced at rated speed is between 25–60% of the nominal torque with guide vanes (wicket gate) closed [2]. In [3], the same is mentioned to be around 22% of the nominal torque with turbine flooded into water. From [4], [5], the torque requirement for a reversible pump-turbine at zero speed can be derived to be 50–125% of the nominal torque at rated speed depending upon the opening of guide vanes.

In [6], it is claimed that full converter is justifiable for pumped storage power plants upto 100 MW of power plants with today's technology. Beyond that capacity, the space occupied by the converter and the cost associated with it push to go for DFIM technology where a smaller converter is required. Therefore, pumped storage hydropower plants with machines in range of hundreds of MW have DFIM to achieve variable speed operation.

A typical synchronous machine in the range of 100 MVA has the stator voltage around 13–15 kV. Therefore, the converter required for CFSM operation should also have the output voltage in the same range. The Load Commutated Inverter (LCI) drives is an existing technology which can supply upto 100 MW but it cannot be considered a proper solution for continuous running as it produces low order harmonic current on both machine and grid side. This results in torque harmonics in the machine and therefore, the solution is limited for starting large machines.

This paper focuses on the converter topology which en-

ables medium-voltage output to facilitate a transformerless connection to the machine. Most importantly, the aim is to find a converter topology that yields a high starting torque in pumping mode and enables a wide range of speed variation.

The remainder of this paper is organized as follows. A brief description of the NPC and ANPC converter topologies, and the overview of available devices are covered in Section II. The analytical equations to calculate conduction and switching losses in the devices of NPC and ANPC are presented in Section III. These are followed by the results of the loss analysis and the comparison in Section IV. Finally, Section VI highlights the major conclusions of this paper.

II. CONVERTER TOPOLOGY

The most popular and matured converter topology in medium voltage industrial drives is NPC topology in MW (upto 30 MVA) power rating. As variable speed operation of pumped storage hydropower plant with full size converter is in the initial phase, the currently available industrial solutions has been adopted. Nonetheless, as the power rating increases, for instance, upto 100 MW, the requirements regarding the starting torque also increases. This is primarily because the combined inertia of the machine shaft and turbine becomes larger for larger hydropower machines. Thus, higher starting torque is the must to accelerate the machine quickly to the rated speed.

A. Neutral Point Clamped Converter

As discussed in [7]–[9], 3-level NPC converter configuration has been the major workhorse in medium–voltage drives application. The schematic of the topology is shown in Fig.1. Many power drives with voltage rating up to 6.6 kV are widely used in industries employing NPC converter topology.
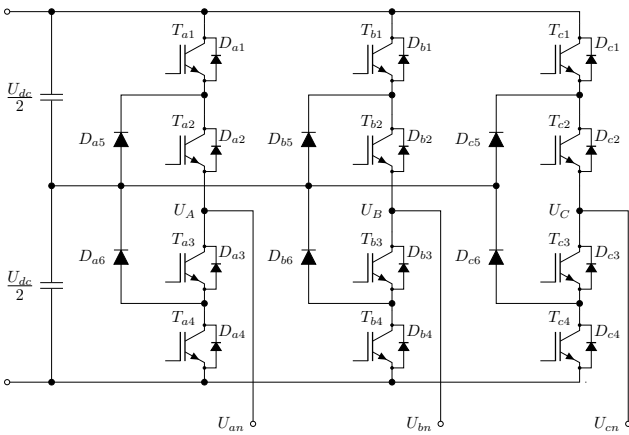

Fig. 1. Schematic of a 3-level 3-phase Neutral Point Clamped (NPC) Converter configuration.

Although NPC converter topology can fulfil the voltage requirement for this application, there is a drawback associated with it regarding loss distribution among the semiconductor devices. In particular, at low speed operation, the clamping diodes (D_5) and (D_6) have higher losses. Therefore, when it is required to operate at low modulation index and low frequency

during start-up, additional switches are added across these diodes to modify the topology, named as ANPC converter topology. The detail comparison is presented in Section IV.

B. Active Neutral Point Clamped Converter

The ANPC converter is a preferred solution over NPC converter where a single converter is required to achieve higher starting torque [10], [11]. The additional two switches across the clamping diodes in each bridge leg share the current flow and hence distribute the losses more evenly compared to that in the NPC converter. The schematic of the topology is presented in Fig.2.

An example of pumped storage hydropower plant with variable speed operation is Grimsel 2 in Switzerland. This plant has a converter of 100 MW installed to one of its units. The solution consists of two parallel ANPC converters connected via transformers to both stator of the machine and grid side transformer [12].
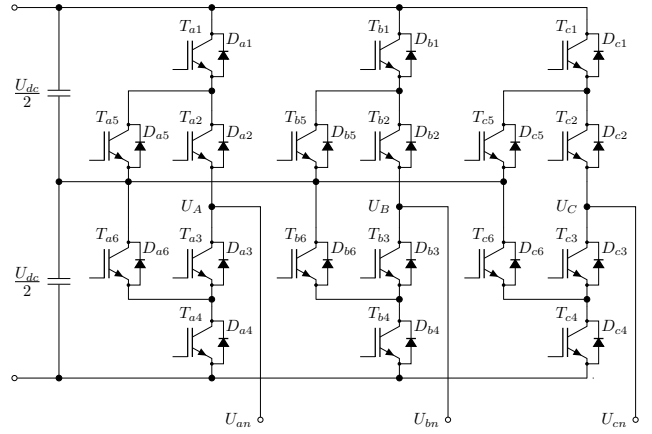

Fig. 2. Schematic of a 3-level 3-phase Active Neutral Point Clamped (ANPC) Converter configuration.

C. Available devices

The devices available in the market at the moment with the highest voltage and current ratings to achieve high voltage and high power with a single converters is presented in Table I.

TABLE I
MARKET OVERVIEW OF HIGH VOLTAGE AND HIGH CURRENT
SEMICONDUCTOR DEVICES [13]–[16]

Manufacturer	Device Type	U_{CE} [V]	U_{dc}^* [V]	Ic [A]
ABB	IGCT (Presspack)	6500	4000	3800
		4500	2800	4500
	BIGT (Presspack)	5200	3400	3000
Westcode	IGBT (Presspack)	6500	3600	900
		4500	2800	3000
Hitachi	IGBT (Presspack)	4500	2800	1500
		6500	3600	750
Toshiba	IEGT (Presspack)	4500	2700	2100

The variables used in the table are: Maximum collector-emitter voltage of the device at 25 °C, U_{CE}; Permanent dc-link voltage, U_{dc}^*; Continuous collector current of the device, I_c. The device acronyms used are: Integrated Gate-Commutated Thyristor, IGCT; Bi-Mode Insulated Gate Transistor, BIGT; Insulated Gate Bipolar Transistor, IGBT; Injection-Enhanced Gate Transistor, IEGT.

The devices with higher voltage ratings are not available with higher currents (e.g. 6500 V IGBTs) or with a matching high current diodes (e.g. 6500 V IGCTs) and thus, it cannot be an ideal selection to meet both high voltage and high power requirements. Therefore, devices with 4500 V have been considered for further evaluation.

D. Converter Configuration for Transformerless Connection

One of the major requirements of a full size converter for pumped storage hydropower plant is the transformerless connection to the machine and grid side transformer. In other words, only the converter should be placed between the step-up transformer (the transformer which connects the machine to the grid) and the synchronous machine.

As the semiconductor devices are rated for their blocking voltage, the dc-link voltage of the converter is necessary to be determined for the ac voltage output of 13–15 kV. The relation between the ac output voltage and the dc-link voltage in a PWM modulated converter is as in (1) [17].

$$U_{ll,peak} = \frac{\sqrt{3}}{2} M \cdot U_{dc} \qquad (1)$$

where, $U_{ll,peak}$ is the peak value of phase-to-phase ac output voltage, U_{dc} is the pole to pole dc-link voltage and M is the peak of sinusoidal modulation index. With space vector PWM modulation or sinusoidal PWM with 3rd harmonics injection technique, modulation index can be increased to $\frac{2}{\sqrt{3}}$ (≈ 1.1547) to achieve maximum output voltage for same dc-link voltage. In this case, the output voltage and dc-link voltage can be related as in (2).

$$U_{ll,peak} = U_{dc} \qquad (2)$$

From (2), the dc-link voltage required for a 13 kV (rms) output is 18.4 kV. Since there are no devices available in this voltage range as listed in Table I, several devices (both switches and diodes) need to be connected in series. As in [18]–[21], a de-rating of 80–85% of the voltage rating of the devices is necessary while connecting several devices in series. Considering this de-rating, the dc-link voltage would be close to 22 kV. From Table I, the device with the highest power ratings can be selected to achieve maximum power rating of the converter. Therefore, if the permanent dc-link voltage (U_{dc}^*) rating of the selected device is 2800 V, at least 4 devices need to connected in series at each position of the converter configuration shown in Fig.2 to block the half of the dc-link voltage. A dv/dt filter can also be required to filter the sharp and large voltage steps to protect the stator winding insulation.

III. ANALYTICAL LOSS CALCULATION

The amplitude and frequency of the stator current change according to the variation in load. This stator current is the same current that flows through the semiconductor devices. In a PWM modulated converter, the current commutates from one device to the other at each PWM pulse which causes switching loss in the devices. A finite value of voltage drop across the devices causes conduction loss when the current flows through

it. The conduction and switching losses in the devices also vary with the change in the load current. Therefore, it is important to identify the worst case loss in each device while dimensioning these components. It is possible to calculate these losses using analytical equations for the devices at each position of the NPC and ANPC converters.

The analytical equations to calculate the conduction and switching losses in each device in a 3-level 3-phase NPC converter is presented in [22]. These equations are used to calculate the losses at different modulation index and different load power factor ($\cos \varphi$) to find the worst case losses in each device of NPC converters. The similar analytical equations for ANPC converters to find the conduction and switching losses in each devices is derived in [23]. These expressions are accurately valid only for PWM modulated converters. The medium–voltage multilevel converters today employ only low switching frequency in the range of 200–500 Hz to avoid high switching loss [24]. Thus, synchronous modulation technique is used to eliminate the low order harmonics in the output voltage. In future, wide-bandgap devices will be available in higher voltage and current ratings than today and can employ higher switching frequency. Then, these expressions can be applied to estimate the losses with very high accuracy.

From Fig. 1 and 2, it can be observed that there is symmetry in the position of the devices looking from the mid-point of each bridge legs. Therefore, analysis of losses in devices: T_1, T_2, D_1, D_2 and D_5 in case of NPC converter and an additional device T_5 in case of ANPC converter would be sufficient.

A. Conduction Loss

The conduction loss in a semiconductor device can be calculated using (3).

$$P_{con,loss} = U_{CE0} \cdot I_{avg} + R_{CE,on} \cdot I_{rms}^2 \qquad (3)$$

where, U_{CE0} is the threshold voltage of the device, $R_{CE,on}$ is on-state resistance and I_{avg} and I_{rms} are the average and rms current flowing through the device over a time period of fundamental frequency component of the output current. From (3), the average and rms current flowing through each device is necessary to find the conduction loss in that particular device. The equations to calculate these currents depending upon the peak of output current ($\hat{I}_o$), modulation index (M) and power factor ($\cos \varphi$) are as follows:

$$I_{T1,avg} = \frac{M\hat{I}_o}{4} \cos \varphi + \frac{M\hat{I}_o}{4\pi} \left(\sin |\varphi| - |\varphi| \cos \varphi \right) \qquad (4)$$

$$I_{D1,avg} = \frac{M\hat{I}_o}{4\pi} \left(\sin |\varphi| - |\varphi| \cos \varphi \right) \qquad (5)$$

$$I_{T1,rms}^2 = \frac{M\hat{I}_o^2}{6\pi} \left(1 + \cos \varphi \right)^2 \qquad (6)$$

$$I_{D1,rms}^2 = \frac{M\hat{I}_o^2}{6\pi} \left(1 - \cos \varphi \right)^2 \qquad (7)$$

The current through the devices T_1 and D_1 in the NPC and ANPC converter configurations are same, therefore, the

average and rms currents and hence, the conduction loss in these devices would be same in both cases.

The similar expressions for the average and rms currents through the devices T_2, D_2 and D_5 are:

$$I_{T2,avg,npc} = \frac{\hat{I}_o}{\pi}\left[1 - \frac{M}{4}\left(\sin|\varphi| - |\varphi|\cos\varphi\right)\right] \tag{8}$$

In NPC converter, diode D_1 and D_2 conduct simultaneously and have same average and rms current flowing through them.

$$I_{D5,avg,npc} = \frac{\hat{I}_o}{\pi}\left[1 - \frac{M}{2}\left(\sin|\varphi| + \left(\frac{\pi}{2} - |\varphi|\right)\cos\varphi\right)\right] \tag{9}$$

$$I_{T2,rms,npc}^2 = \frac{\hat{I}_o^2}{4}\left[1 - \frac{2M}{3\pi}(1 - \cos\varphi)^2\right] \tag{10}$$

$$I_{D5,rms,npc}^2 = \frac{\hat{I}_o^2}{4}\left[1 - \frac{4M}{3\pi}\left(1 + \cos^2\varphi\right)\right] \tag{11}$$

For ANPC converter, the expressions to calculate the average and rms current through the devices T_2, D_2, T_5 and D_5 are:

$$I_{T2,avg,anpc} = \frac{\hat{I}_o}{2\pi}\left[1 + \frac{\pi}{4}M\cos\varphi\right] \tag{12}$$

$$I_{D2,avg,anpc} = \frac{\hat{I}_o}{2\pi}\left[1 - \frac{\pi}{4}M\cos\varphi\right] \tag{13}$$

$$I_{D5,avg,anpc} = \frac{\hat{I}_o}{2\pi}\left[1 - \frac{M}{2}\left(\sin|\varphi| + \left(\frac{\pi}{2} - |\varphi|\right)\cos\varphi\right)\right] \tag{14}$$

$$I_{T2,rms,anpc}^2 = \frac{\hat{I}_o^2}{4}\left[\frac{1}{4} + \frac{M}{3\pi}\left(1 + \cos^2\varphi + 4\cos\varphi\right)\right] \tag{15}$$

$$I_{D2,rms,anpc}^2 = \frac{\hat{I}_o^2}{4}\left[\frac{1}{4} + \frac{M}{3\pi}\left(1 + \cos^2\varphi - 4\cos\varphi\right)\right] \tag{16}$$

$$I_{D5,rms,anpc}^2 = \frac{\hat{I}_o^2}{16}\left[1 - \frac{4M}{3\pi}\left(1 + \cos^2\varphi\right)\right] \tag{17}$$

B. Switching Loss

The switching loss in the devices of a 3-level 3-phase NPC or ANPC converter does not depend on the modulation index as it does not influence the number of switching over one cycle but the load power factor ($\cos\varphi$) does. The power factor other than unity makes the load current lead/lag the modulation index and the current is shared between the switches and the anti-parallel diodes across them.

The switching loss characteristics as function of current, $e_{sw}(i)$, from an experimental result can be approximated as in (18).

$$e_{sw}(i) = k_{1,T}\cdot i + k_{2,T}\cdot i^2 \tag{18}$$

where, $k_{1,T}$ and $k_{2,T}$ are the curve fitting coefficients determined using the experimental results or manufacturer's datasheet. The same coefficients for diodes are $k_{1,D}$ and $k_{2,D}$.

Using these coefficients, the expressions for calculating the switching loss in each devices can be formulated.

$$P_{T1,sw,npc} = \frac{U_{dc}}{2U_{dc}^*}\frac{\hat{I}_o}{2\pi}f_{sw}\left[k_{1,T}\left(1 + \cos\varphi\right)\right.$$
$$\left. + \frac{\hat{I}_o}{2}k_{2,T}\left(\pi - |\varphi| + \frac{1}{2}\sin 2|\varphi|\right)\right] \tag{19}$$

$$P_{D1,sw,npc} = \frac{U_{dc}}{2U_{dc}^*}\frac{\hat{I}_o}{2\pi}f_{sw}\left[k_{1,D}\left(1 - \cos\varphi\right)\right.$$
$$\left. + \frac{\hat{I}_o}{2}k_{2,D}\left(|\varphi| - \frac{1}{2}\sin 2|\varphi|\right)\right] \tag{20}$$

The equation for switching loss in devices T_1 and D_1 in ANPC converter is same as that in NPC converter. Therefore, (19) and (20) are valid for ANPC converter as well.

$$P_{T2,sw,npc} = \frac{U_{dc}}{2U_{dc}^*}\cdot\frac{\hat{I}_o}{2\pi}f_{sw}\left[k_{1,T}\left(1 - \cos\varphi\right)\right.$$
$$\left. + \frac{\hat{I}_o}{2}k_{2,T}\left(|\varphi| - \frac{1}{2}\sin 2|\varphi|\right)\right] \tag{21}$$

In case of ANPC converter, $\hat{I}_o$ is replaced by $\hat{I}_o/2$ in (21) to calculate the switching loss in the switches T_2 and T_5.

$$P_{D2,sw,npc} = 0 \tag{22}$$

$$P_{D5,sw,npc} = \frac{U_{dc}}{2U_{dc}^*}\frac{\hat{I}_o}{2\pi}f_{sw}\left[k_{1,D}\left(1 + \cos\varphi\right)\right.$$
$$\left. + \frac{\hat{I}_o}{2}k_{2,D}\left(\pi - |\varphi| + \frac{1}{2}\sin 2|\varphi|\right)\right] \tag{23}$$

For the devices in ANPC converter, $\hat{I}_o$ is replaced by $\hat{I}_o/2$ in (23) to find the switching loss in the diodes D_2 and D_5.

IV. RESULTS

In this section, the total loss in each semiconductor devices in NPC and ANPC converters is calculated at rated speed operation and zero speed operation using the expressions mentioned in Section III. The total loss in each device in a converter is the sum of average conduction loss and average switching loss in that device over one fundamental cycle. Mathematically, it can be expressed as in (24).

$$P_{tot} = P_{con} + P_{sw} \tag{24}$$

For the analysis of losses in both NPC and ANPC converter, the IGCT from ABB (5SHY 45L4520) from Table I and the corresponding diode (FRD 5SDF 28L4520) are selected. The IGBTs have higher switching loss compared to IGCTs at the same switching frequency, and therefore, are not favoured for this analysis. The key electrical parameters of the selected switch and diode for loss analysis are presented in Table II. The switching frequency (f_{sw}) is chosen as 250 Hz and dc-link voltage is selected as 5.6 kV such that the $\frac{U_{dc}}{2U_{dc}^*}$ ratio is 1. The analysis is done assuming same type of switches and diodes at each position in the converters.

Parameters	Values
On-state Knee Voltage of IGCT (U_{CE0})	1.84 V
On-state Resistance of IGCT ($R_{CE,on}$)	0.73 $m\Omega$
On-state Knee Voltage of Diode (U_{F0})	2.036 V
On-state Resistance of Diode (R_d)	0.33 $m\Omega$

A. Rated Speed Operation

The total loss at varying modulation index and power factor have been calculated for each device using the expressions (3)–(24). The distribution of loss in the IGCT 5SHY 45L4520 positioned as T_2 in NPC and ANPC converters are shown in Fig. 3 and 4 respectively and the worst case losses are 3.58 kW and 2.36 kW. Similar analysis has been carried out for all devices and the worst case losses both type of converters while running at rated frequency are presented in Fig. 5. From the figure, the devices T_2 and D_5 for NPC have the maximum losses of 3.66 kW and 4.45 kW respectively. The same in devices T_1 and D_1 for ANPC converter have 3.18 kW and 4.08 kW respectively. These devices with maximum losses at rated speed operation are selected as reference devices for the respective converters.
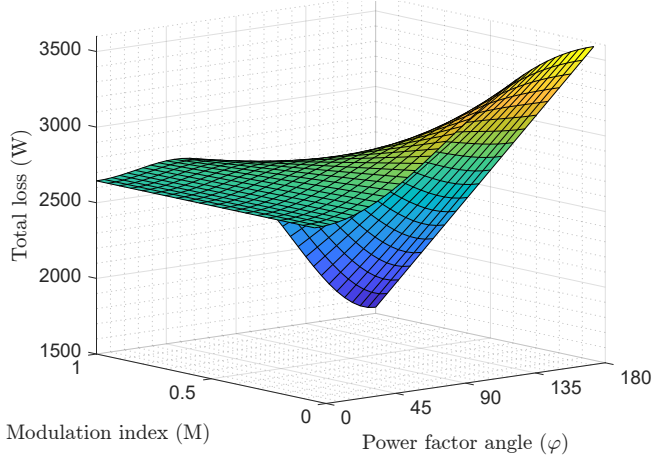

Fig. 3. Loss in switch T_2 in an NPC converter with varying modulation index and power factor angle (φ) at switching frequency (f_{sw}) = 250 Hz. The device used is ABB IGCT 5SHY 45L4520. For device T_2, the worst case loss occurs at $M = 0.05$, $\varphi = 180^o$, i.e. $\cos\varphi = -1$ which is equivalent to running in generating mode at unity power factor. The total loss at this point is 3.58 kW.

B. Zero Speed Operation

All semiconductor devices have either maximum conduction loss or maximum switching loss or both at zero speed. The devices stressed by both type of losses decide the current limit the converter can provide at start-up of the machine. The total loss in the devices increases by a big margin at dc operation. The worst case losses in devices at each position of both NPC and ANPC converters at zero speed are presented in Fig. 6.

At 60% of $\hat{I}_o$, the total loss in diode D_5 of ANPC converter is similar to the total loss at rated frequency in the reference
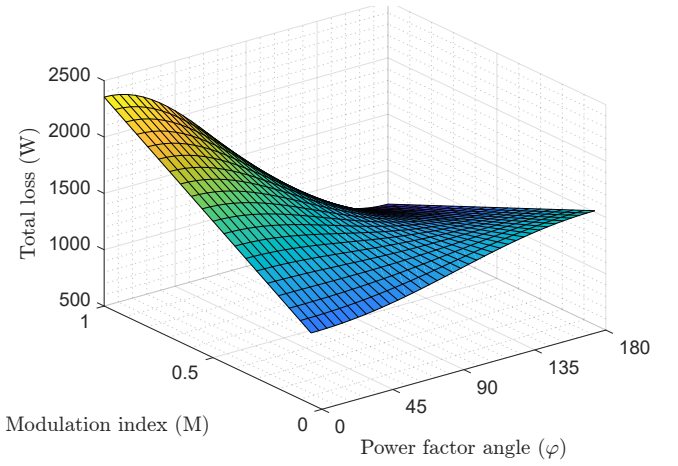

Fig. 4. Loss in switch T_2 in an ANPC converter with varying modulation index and power factor angle (φ) at switching frequency (f_{sw}) = 250 Hz. The device used is ABB IGCT 5SHY 45L4520. For device T_2, the worst case loss occurs at $M = 1$, $\varphi = 0$, i.e. $\cos\varphi = 1$ which is equivalent to running at full load in motoring mode at unity power factor. The total loss at this point is 2.36 kW.
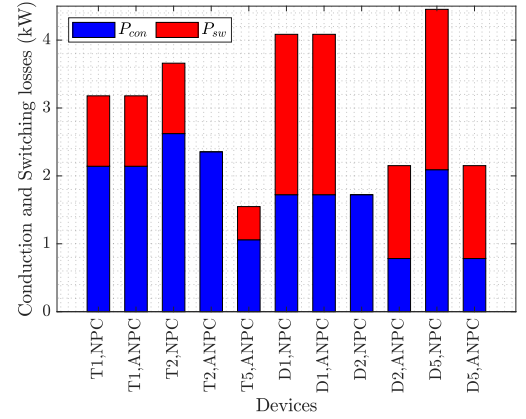

Fig. 5. Worst case losses in each device of NPC and ANPC converters at $\hat{I}_o = 3000A$, $f_n = 50Hz$ and switching frequency (f_{sw}) = 250 Hz. The devices used are ABB IGCT 5SHY 45L4520 and ABB FRD 5SDF 28L4520. The legends used are Conduction loss, P_{con} and Switching loss, P_{sw}. The total loss in the device D_5 in NPC converter and D_1 in ANPC converter are the highest, and are considered as reference devices for respective converters while dimensioning the devices.

device D_1 as shown in Fig. 7. The remaining devices have losses well below the reference devices. But, the loss in the devices T_2 and D_5 of NPC converter are still higher than the reference value. It means in case of NPC, the dc current should further be reduced to keep the losses within the limit. The loss in all the devices in NPC converter are within the limit when the dc current is about 33% of full load current at rated speed.

From this observation, it can be confirmed that the NPC converter can withstand only 33% of full load current at zero speed whereas the same value approaches around 60% in case of the ANPC converter with the selected devices. Thus, ANPC becomes preferable choice for an application where high starting torque is required. This torque at zero speed can further increase if the switching loss in the devices are lower or the devices are stressed to its maximum thermal limit.
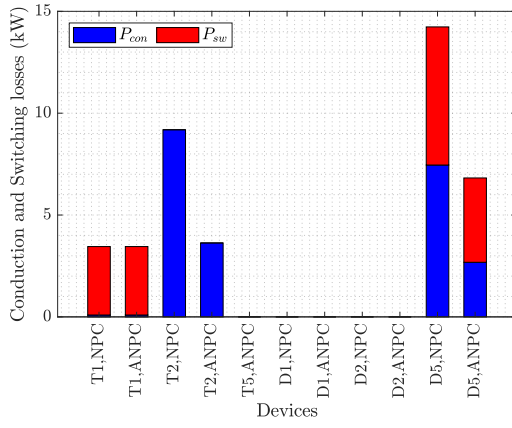
Fig. 6. Worst case losses in each devices of NPC and ANPC converters at $\hat{I}_o = 3000A$, $f_n = 0\ Hz$ and switching frequency (f_{sw}) = 250 Hz. The current is out of the converter bridge leg to run the machine as motor (in this application, the case is starting the machine in pumping mode). The devices D_1 and D_2 in NPC case and D_1, D_2 and T_5 in ANPC case do not conduct for positive dc current and therefore the loss is zero for these devices. The devices used are ABB IGCT 5SHY 45L4520 and ABB FRD 5SDF 28L4520.
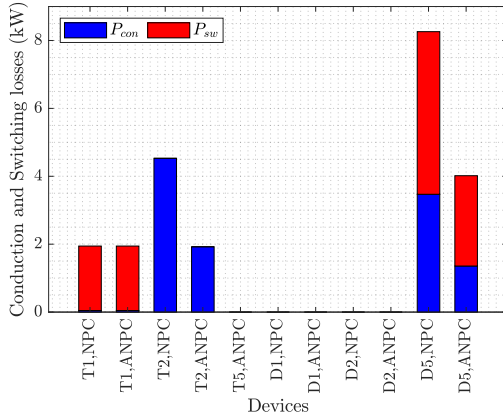

Fig. 7. Worst case losses in each devices of NPC and ANPC converters at $\hat{I}_o = 1800A$, $f_n = 0\ Hz$ and switching frequency (f_{sw}) = 250 Hz. The current is out of the converter bridge leg to run the machine as motor. The devices used are ABB IGCT 5SHY 45L4520 and ABB FRD 5SDF 28L4520.

V. CONCLUSION

On the basis of analysis using analytical equations, this paper shows that ANPC converter can provide 60% of full load torque at standstill, while the NPC converter can deliver only 33% for the same condition with the selected IGCTs as switching devices. As the higher starting torque is one of the major requirements of a pumped storage hydropower plant for fast start-up, ANPC converter is a promising topology over NPC.

In addition, in ANPC converter, the current is shared amongst the inner active switches and diodes, thus the total loss is lower and distributed over more devices compared to the NPC converter. This eases the cooling requirement for ANPC over NPC configuration.

ACKNOWLEDGMENT

REFERENCES

[1] H. Kolstad, "Control of an Adjustable Speed Hydro utilizing Field Programmable Devices," Ph.D. Thesis, NTNU, Norway, 2003.
[2] T. J. Hammons and J. Loughran, "Starting methods for generator/motor units employed in pumped-storage stations," Proceedings of the Institution of Electrical Engineers, vol. 117, no. 9, pp. 1829–1840, Sep. 1970.
[3] M. Canay, "Asynchronous Starting of a 230 MVA Synchronous Machine in 'Vianden 10' Pumped Storage Station," Brown Boveri Rev., vol. 61, no. 7, pp. 313–318, Jul. 1974.
[4] S. Pejovic and B. Karney, "Guidelines for transients are in need of revision," IOP Conf. Ser.: Earth Environ. Sci., vol. 22, no. 4, p. 042006, Mar. 2014.
[5] M. F. Svarstad, "Fast Transition between Operational Modes of a reversible Pump-Turbine", PhD Thesis, NTNU, Norway, 2019.
[6] Ø. J. Linnebo, "Turtallstyring og lastkontroll av pumpeaggregater," presented at the Produksjonsteknisk konferanse (PTK), 2013.
[7] H. Abu-Rub, J. Holtz, J. Rodriguez, and G. Baoming, "Medium-Voltage Multilevel Converters—State of the Art, Challenges, and Requirements in Industrial Applications," IEEE Transactions on Industrial Electronics, vol. 57, no. 8, pp. 2581–2596, Aug. 2010.
[8] D. Krug, S. Bernet, S. S. Fazel, K. Jalili, and M. Malinowski, "Comparison of 2.3-kV Medium-Voltage Multilevel Converters for Industrial Medium-Voltage Drives," IEEE Transactions on Industrial Electronics, vol. 54, no. 6, pp. 2979–2992, Dec. 2007.
[9] J. Rodriguez, S. Bernet, P. K. Steimer, and I. E. Lizama, "A Survey on Neutral-Point-Clamped Inverters," IEEE Transactions on Industrial Electronics, vol. 57, no. 7, pp. 2219–2230, Jul. 2010.
[10] P. Barbosa, P. Steimer, J. Steinke, M. Winkelnkemper, and N. Celanovic, "Active-neutral-point-clamped (ANPC) multilevel converter technology," in 2005 European Conference on Power Electronics and Applications, Sep. 2005, pp. 10.
[11] T. Bruckner, S. Bernet, and P. K. Steimer, "The active NPC converter for medium-voltage applications," in Fourtieth IAS Annual Meeting. Conference Record of the 2005 Industry Applications Conference, 2005., Oct. 2005, vol. 1, pp. 84-91.
[12] H. Schlunegger and A. Thöni, "100MW full-size converter in the Grimsel 2 pumped-storage plant," Innsbruck, Hydro, 2013.
[13] "Asymmetric and reverse conducting Integrated gate-commutated thyristors (IGCT), ABB." https://new.abb.com/semiconductors/integrated-gate-commutated-thyristors-(igct)/asymmetric.
[14] "IXYS UK Westcode - Press-pack IGBT Capsules." http://www.westcode.com/igbt1.html.
[15] "Hitachi — IGBT Product Lineup." http://pdd.hitachi.eu/igbts/4500v.
[16] "Press-Pack package, Toshiba Electronic Devices & Storage Corporation." https://toshiba.semicon-storage.com/ap-en/semiconductor/product/high-power-devices/iegt-ppi/press-pack-package.html.
[17] N. Mohan, T. M. Undeland, and W. P. Robbins, Power Electronics: Converters, Applications, and Design, 3rd Edition, Chapter-8, Wiley, 2002.
[18] M. Bruckmann, R. Sommer, M. Fasching, and J. Sigg, "Series connection of high voltage IGBT modules," in Conference Record of 1998 IEEE Industry Applications Conference. Thirty-Third IAS Annual Meeting, Oct. 1998, vol. 2, pp. 1067–1072.
[19] P. R. Palmer, H. S. Rajamani, and N. Dutton, "Experimental comparison of methods of employing IGBTs connected in series," IEE Proceedings - Electric Power Applications, vol. 151, no. 5, pp. 576–582, Sep. 2004.
[20] Soonwook Hong, Venkatesh Chitta, and D. A. Torrey, "Series connection of IGBT's with active voltage balancing," IEEE Transactions on Industry Applications, vol. 35, no. 4, pp. 917–923, Jul. 1999.
[21] I. Baraia, J. A. Barrena, G. Abad, J. M. Canales Segade, and U. Iraola, "An Experimentally Verified Active Gate Control Method for the Series Connection of IGBT/Diodes," IEEE Transactions on Power Electronics, vol. 27, no. 2, pp. 1025–1038, Feb. 2012.
[22] G. Tomta and R. Nilsen, "Analytical Equations for Three Level NPC Converters," in 9th European Conference on Power Electronics and Applications, Graz, 2001.
[23] R. Tiwari and R. Nilsen, "Analytical Loss Equations for Three Level Active Neutral Point Clamped Converters," IECON 2020 - 46th Annual Conference of the IEEE Industrial Electronics Society, Singapore, 2020, "unpublished".
[24] J. Rodriguez et al., "Design and Evaluation Criteria for High Power Drives," in 2008 IEEE Industry Applications Society Annual Meeting, Oct. 2008, pp. 1–9.